SCIENTIFIC REPORTS
nature research

Check for updates

OPEN

Redox-active, luminescent coordination nanosheet capsules containing magnetite

Ryo Arai[1], Mengjuan Li[1,2], Ryojun Toyoda[1], Hiroaki Maeda[1,3] & Hiroshi Nishihara[1,3]✉

Two-dimensional coordination nanosheets (CONASHs) are grown at the spherical liquid–liquid interface of a dichloromethane droplet in water to form zero-dimensional nano- and micro-capsules using a simple dropping method, a syringe-pump method, and an emulsion method. Reaction of 1,3,5-tris[4-(4′-2,2′:6′,2″-terpyridyl)phenyl]benzene (1) with $Fe(BF_4)_2$ affords electrochromic $Fe(tpy)_2$ CONASH capsules and that of ligand 1 with $ZnSO_4$ does photoluminescent $Zn_2(\mu\text{-}O_2SO_2)_2(tpy)_2$ CONASH capsules. $Fe(tpy)_2$ CONASH capsules containing magnetite particles were produced by the syringe-pump method by adding magnetite to the aqueous phase, with the assembly and dispersion of the magnetite-containing CONASH capsules being easily controlled with a magnet. This indicates that physicochemically functional CONASH capsules are suitable for incorporating other functional materials to develop hybrid systems.

Two-dimensional (2D) materials such as graphene[1,2] and transition-metal dichalcogenides[3,4], have unique properties and functions for various applications[5–8]. Coordination nanosheets (CONASHs) are 2D materials that consist of metal ions and organic π-ligands[9,10]. Since the discovery of an electronically conducting bis(dithiolato)nickel nanosheet[11], a range of CONASHs have been synthesized and various physical properties such as electronic conductivity[12,13], energy storage[14], redox activity[15], luminescence[16], photoelectric conversion[17], and electrocatalytic activity[18] have been enhanced by tuning the chemical structures. Films can be directly synthesized by a reaction at the liquid–liquid or gas–liquid interface, where metal ions and organic ligands exist in different phases. Most previous work on CONASHs has used planar interfaces to obtain planar films; however, other spherical functional nanomaterials have been extensively studied[19–31].

In this study, we used the spherical liquid–liquid interface of droplets to synthesize spherical CONASHs focusing on their functions. Using 1,3,5-tris[4-(4′-2,2′:6′,2″-terpyridyl)phenyl]benzene (**1**), which is a three-way bridging tris(terpyridine) ligand, we obtained electrochromic $Fe(tpy)_2$[32–34] CONASH capsules and photoluminescent $Zn_2(SO_4)_2(tpy)_2$[16,35] CONASH capsules by a simple dropping method, a syringe pump method and an emulsion method. The formation of the CONASHs at the liquid–liquid interfaces is accelerated by the addition of surfactant such as sodium dodecyl sulfate (SDS), allowing the CONASH capsules to be formed within 15 min[36,37]. The surfactant also stabilizes the droplets during synthesis[38,39]. We also encapsulated magnetite (Fe_3O_4) particles[40] in the $Fe(tpy)_2$ shell, and the magnetite-containing $Fe(tpy)_2$ CONASH capsules could be controlled with a magnet. Our results show that physicochemically functional CONASH capsules are suitable for incorporating other functional materials to develop hybrid systems.

Synthesis of electrochromic $Fe(tpy)_2$ CONASH capsules using the dropping method. We previously synthesized a planar $Fe(tpy)_2$ CONASH film (Fig. 1a) using the coordination reaction at the planar interface between $Fe(BF_4)_2$ in water and the tris(terpyridine) ligand, **1**. The reaction was sluggish and took several hours to grow a film of sub-micron thickness. The reaction to fabricate CONASH capsules occurs at the spherical liquid–liquid interface between an aqueous phase containing metal ions and an organic phase containing organic ligands (Fig. 1b). Because the reaction is slow, the droplets easily fuse (Fig. 1c I). Adding a surfactant, such as SDS, accelerated the coordination reaction at the interface, shortening the reaction time to 15 min (Fig. 1c II). To grow the $Fe(tpy)_2$ capsules with a shell thickness of 20 nm (Supplementary Fig. S1),

[1]Department of Chemistry, School of Science, The University of Tokyo, 7-3-1 Hongo, Bunkyo-ku, Tokyo 113-0033, Japan. [2]College of Textile Science and Engineering, Jiangnan University, Wuxi, Jiangsu, China. [3]Research Center for Science and Technology, Tokyo University of Science, 2641 Yamazaki, Noda, Chiba 278-8510, Japan. ✉email: nisihara@rs.tus.ac.jp

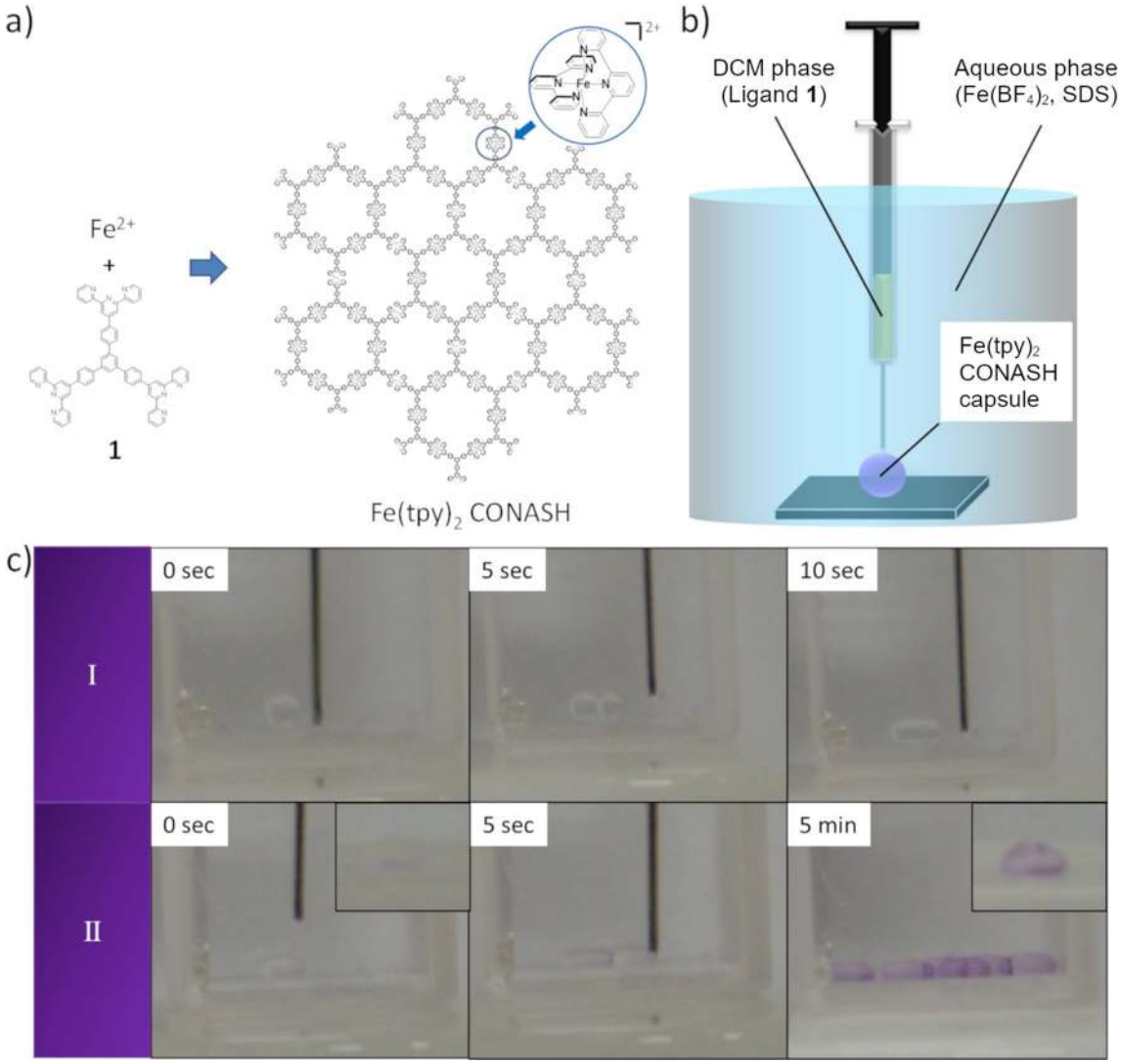

Figure 1. Dropping method to form $Fe(tpy)_2$ CONASH capsules. (**a**) Chemical structure of $Fe(tpy)_2$ CONASH. (**b**) Conceptual image of dropping method. (**c**) Snapshots of $Fe(tpy)_2$ CONASH capsules fabricated by dropping method, (I) in the absence of surfactant and (II) in the presence of SDS.

droplets of ligand **1** in dichloromethane (DCM) were created in an aqueous solution of $Fe(BF_4)_2$. Due to the fast reaction, $Fe(tpy)_2$ capsules were fabricated without the droplets fusing. Amphiphilic SDS makes a metal complex with a ferrous ion in an aqueous phase. The formed complex easily moves to organic phase and works as an iron ion source of $Fe(tpy)_2$ complex. Hence, SDS can work as an accelerator of the complexation reaction of $Fe(tpy)_2$ complex at the organic-water solution interface.

The characterization of the $Fe(tpy)_2$ capsules was conducted using UV–Vis and Raman spectra. The capsule gives a peak derived from MLCT of $Fe(tpy)_2$ complex at 580 nm corresponding with that of $Fe(tpy)_2$ nanosheet (Fig. 2a). In addition, Raman spectra of $Fe(tpy)_2$ capsule and nanosheet show good agreement each other (Fig. 2b). These spectroscopic results suggest that the capsule is composed of $Fe(tpy)_2$ nanosheet which was formed at the spherical liquid–liquid interface. In the simple dropping method using a micro-syringe, the place and size of the spherical capsules in the size range 1–2.5 mm were easily controlled (Supplementary Fig. S2).

Cyclic voltammetry of a single $Fe(tpy)_2$ CONASH capsule 0.95 mm in diameter on an indium–tin oxide (ITO) glass plate was performed in 0.1 M Na_2SO_4 aq (Fig. 2c, Supplementary Fig. S3). Small oxidation and re-reduction peaks derived from the redox reaction of $[Fe(tpy)_2]^{3+/2+}$ appeared at 1.10 and 0.98 V (vs. Ag/AgCl) and thus $E^{0'} = 1.04$ V (vs. Ag/AgCl) with a peak-to-peak potential of 120 mV, indicating a chemically reversible, slow electron-transfer process, probably because of the weak physical contact between the droplet and ITO.

We previously reported that the planar $Fe(tpy)_2$ CONASH film on an ITO electrode undergoes rapid and durable electrochromism[34]; the color changed reversibly between purple and pale yellow for $[Fe(tpy)_2]^{2+}$ and $[Fe(tpy)_2]^{3+}$, respectively. In the present study, we observed a similar color change (Fig. 2d), although the color was faint because the $Fe(tpy)_2$ shell was thin. The color of the whole shell changed, even though the contact area of the CONASH capsule with the electrode was very small indicating rapid electron hopping between $Fe(tpy)_2$ sites through the molecular framework of the shell.

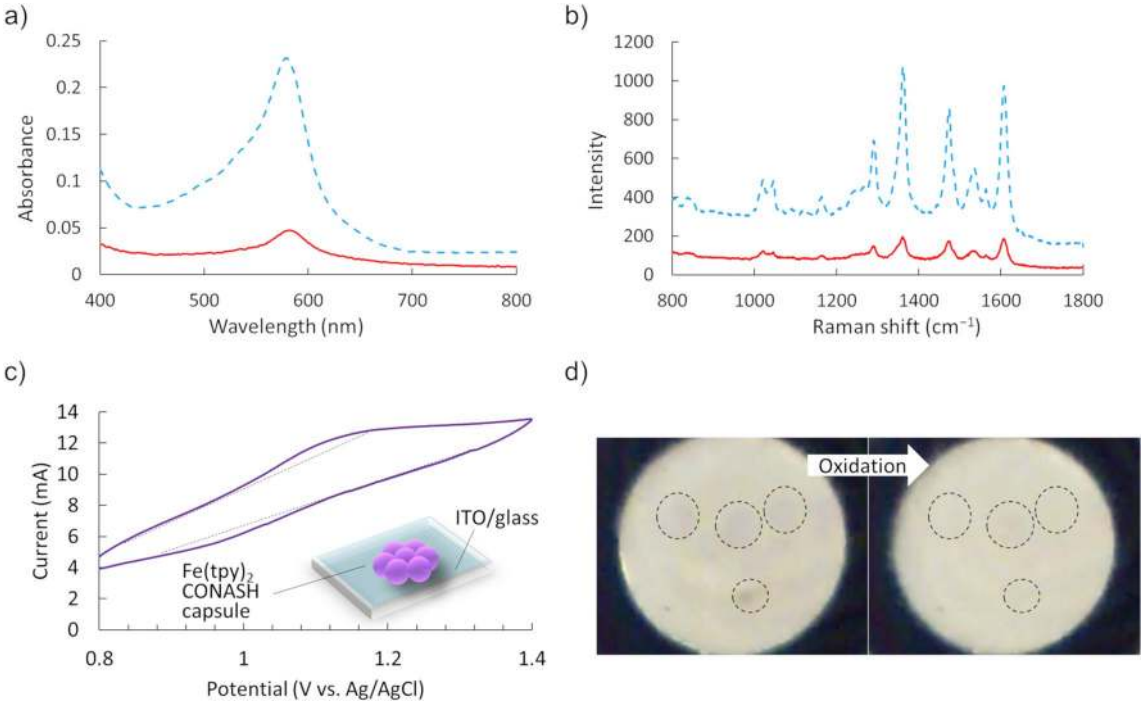

Figure 2. Electrochemical and spectral properties. (**a**) UV–Vis absorption spectra of $Fe(tpy)_2$ CONASH capsules (solid line) and a CONAH film (broken line). (**b**) Raman spectra of $Fe(tpy)_2$ CONASH capsules (solid line) and a CONASH film (broken line). (**c**) Cyclic voltammogram of $Fe(tpy)_2$ CONASH capsules and schematic of the capsules on an ITO electrode. (**d**) Images of $Fe(tpy)_2$ CONASH capsules oxidized electrochemically. (**b**) Cyclic voltammogram of $Fe(tpy)_2$ CONASH capsules and schematic of the capsules on an ITO electrode.

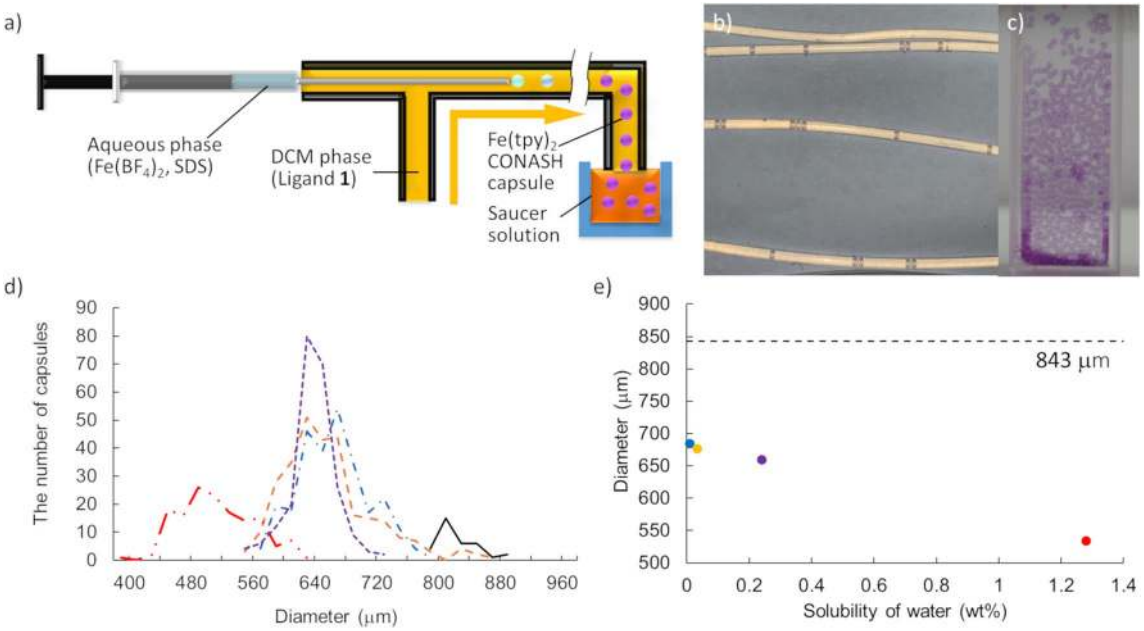

Figure 3. Syringe-pump method to form $Fe(tpy)_2$ CONASH capsules. (**a**) Schematic of the syringe-pump method. (**b**) Photograph of $Fe(tpy)_2$ CONASH capsules during the formation in tubes. (**c**) Photograph of $Fe(tpy)_2$ CONASH capsules in hexane. (**d**) Size distribution of $Fe(tpy)_2$ CONASH capsules in the tube (solid line) and saucer organic solvents; diethyl ether (two-dot chain line), DCM (dotted line), toluene (broken line), and hexane (chain line). (**e**) Diameter of $Fe(tpy)_2$ CONASH capsules vs. solubility of water in a given organic solvent; diethyl ether (red), DCM (purple), toluene (orange), and hexane (blue). The diameter in the tube, 843.2 μm is given for comparison.

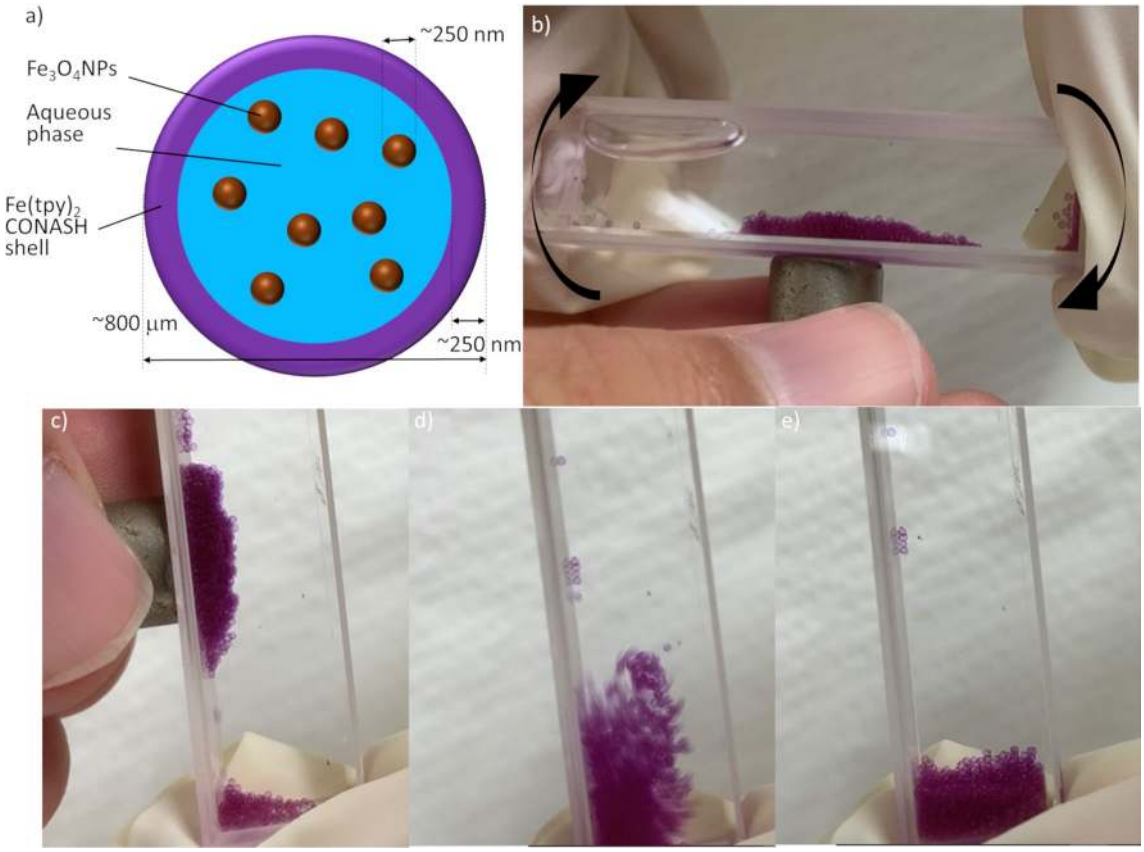

Figure 4. Magnetite-containing $Fe(tpy)_2$ CONASH capsules. (**a**) Schematic of magnetite-containing $Fe(tpy)_2$ CONASH capsules. (**b–e**) Snapshots of the magnetite-containing $Fe(tpy)_2$ CONASH capsules attracted by a magnet.

Synthesis of $Fe(tpy)_2$ CONASH capsules using the syringe-pump method and encapsulation of magnetite particles. The syringe-pump method, in which water droplets are formed and flow continuously in the moving organic solution, was used to obtain $Fe(tpy)_2$ CONASH capsules with a narrow size distribution, easily and constantly (Fig. 3a). The size of the droplets depended on the radius of tubes[41,42], while the flow rate and tube length controlled the reaction time at the liquid–liquid interface, and thus the thickness of the $Fe(tpy)_2$ shells (Fig. 3b). $Fe(tpy)_2$ CONASH capsules were collected at the end of the tube in a saucer solution (Fig. 3a,c). We synthesized $Fe(tpy)_2$ CONASH capsules using DCM as the organic phase of the reaction. Capsules with a diameter of 843 ± 28 μm and a shell thickness of 250 nm were obtained under typical conditions involving 25 mM $Fe(BF_4)_2$; 10 mM SDS; aqueous solution flow rate of 0.5 mL h^{-1}; syringe inner diameter 0.15 mm; 60 μM ligand **1**; DCM solution flow rate 10 mL h^{-1}, and tube inner diameter 0.86 mm (Supplementary Fig. S4). Capsule size depended on the saucer solution, and was 659 ± 29 μm in DCM, 684 ± 44 μm in hexane, 677 ± 57 μm in toluene, and 534 ± 48 μm in diethyl ether (Fig. 3d,e, Supplementary Fig. S5). The diameter of $Fe(tpy)_2$ CONASH capsules was thus expected to depend on the solubility of water in the saucer solvent; larger in hydrophobic solvents than in hydrophilic solvents. In hydrophilic solvents, water dissolved in the outer organic solvents and was transferred out of the $Fe(tpy)_2$ shell. This dependency of capsule size on the outer environment suggests that the capsules might have the permeability of water due to the porous structures of $Fe(tpy)_2$ CONASH.

The space in $Fe(tpy)_2$ CONASH capsules could be used to add further functionality. Magnetic particles and beads have been used for various applications in fields such as biomedical engineering and heterogeneous catalysis because their aggregation and dispersion are easily controlled by an external magnetic field. We introduced magnetite (Fe_3O_4) particles into CONASH capsules by a simple syringe-pump method. Magnetite particles with a diameter of 250 nm[40] were dispersed in an aqueous solution of $Fe(BF_4)_2$. The $Fe(tpy)_2$ CONASH capsules emerged at the water–DCM interface and contained the magnetite particles (Fig. 4a). This method of assembly of CONASH capsules could be controlled externally. The magnetite-containing CONASH capsules were strongly attracted by magnets (Fig. 4b–e), demonstrating that the $Fe(tpy)_2$ CONASH capsules showed the functionality of the original $Fe(tpy)_2$ CONASH shell and the incorporated magnetite.

Synthesis of photoluminescent $Zn_2(SO_4)_2(tpy)_2$ CONASH capsules. We previously reported that the liquid–liquid interfacial coordination reaction of a DCM solution of ligand **1** and an aqueous solution of $ZnSO_4$ produces a photoluminescent sulfate-bridged dimeric zinc terpyridine complex polymer film called $Zn_2(SO_4)_2(tpy)_2$ CONASH (Fig. 5a)[16]. Therefore, we investigated the synthesis of $Zn_2(SO_4)_2(tpy)_2$ CONASH capsules using not only the dropping method but also the emulsion method, in which a DCM solution of ligand **1**

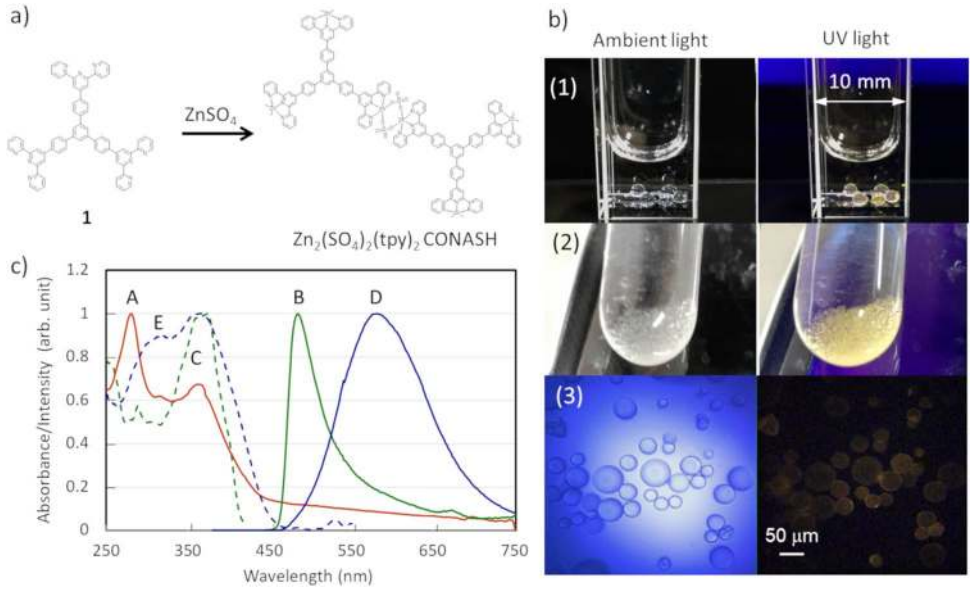

Figure 5. $Zn_2(SO_4)_2(tpy)_2$ CONASH capsules. (**a**) Synthesis of $Zn_2(SO_4)_2(tpy)_2$ CONASH capsules. (**b**) Photographs and microscope images of $Zn_2(SO_4)_2(tpy)_2$ CONASH capsules obtained by the dropping method (1) and by the emulsion method (2, 3) under ambient and 365 nm UV light. (**c**) Absorption (A), emission (B) and excitation (C) spectra of $Zn_2(SO_4)_2(tpy)_2$ CONASH capsules in DCM, and emission (D) and excitation (E) spectra of $Zn_2(SO_4)_2(tpy)_2$ CONASH capsules in water.

and an aqueous solution of $ZnSO_4$ (1:3 v/v) were shaken together vigorously in a test tube to obtain an emulsion. The emulsion interface was left to stand for 1 h, and $Zn_2(SO_4)_2(tpy)_2$ CONASH formed at the interface as a transparent film (Fig. 5b). Note that in the case of the emulsion method, shaking a mixture of the dichloromethane solution and the aqueous solution in a test tube makes smaller microcapsules than those produced by the other methods. We think they have sufficiently large surface area so that the interfacial reaction proceeds rapidly even without adding SDS. The $Zn_2(SO_4)_2(tpy)_2$ CONASH capsules were 20–50 μm in size, showed UV absorption bands at 372 and 281 nm in DCM and exhibited solvatoluminochromism[16]; pale yellow-green photoluminescence with an emission maximum at 580 nm in water and pale blue photoluminescence with an emission maximum at 484 nm in DCM upon UV irradiation (365 nm) (Fig. 5c).

Conclusions

We produced CONASH capsules from 2D coordination polymers using the spherical liquid–liquid interface of DCM droplets in water. The simple dropping method, the syringe-pump method, and the emulsion method were used to synthesize $Fe(tpy)_2$ CONASH capsules and $Zn_2(SO_4)_2(tpy)_2$ CONASH capsules. The $Fe(tpy)_2$ CONASH capsules retained the electrochromism of the nanosheet and the $Zn_2(SO_4)_2(tpy)_2$ CONASH capsules retained the photoluminescence. The syringe-pump method incorporated magnetite into the $Fe(tpy)_2$ CONASH capsules by mixing magnetite in the aqueous phase. The assembly and dispersion of the capsules could be controlled by a magnet. Our results demonstrate that the application range of CONASHs can be expanded by using a zero-dimensional material instead of a 2D material.

Methods

Synthesis of $Fe(tpy)_2$ CONASH capsules by the dropping method. A DCM solution of ligand **1**[33,43] (60 μM) and an aqueous solution containing 25 mM $Fe(BF_4)_2$ and saturated SDS were prepared. The aqueous solution (10 mL) was poured into a vial. A droplet of DCM solution (1 μL) was placed in the aqueous solution by slow pipetting. After 15 min, the purple $Fe(tpy)_2$ CONASH sphere emerged at the interface. Some measurements were conducted in situ or the sphere was removed with the substrate and washed with deionized water, ethanol, and DCM.

Synthesis of $Fe(tpy)_2$ CONASH capsules by the syringe pump method. A DCM solution of the ligand **1** (60 μM) and an aqueous solution containing 25 mM $Fe(BF_4)_2$ and saturated SDS were prepared. The aqueous phase was injected through a hollow needle (25 s gauge, 90° tip, inner diameter of 0.15 mm, outer diameter at the tip of 0.51 mm) in a co-floating stream of the DCM phase floating through polytetrafluoroethylene tubing (inner diameter 0.86 mm). The $Fe(tpy)_2$ CONASH capsules were collected and kept in organic solvent. The aqueous and DCM phases were both supplied by syringe pump set at 0.5 and 10 mL h^{-1}, respectively.

Synthesis of $Zn_2(SO_4)_2(tpy)_2$ CONASH capsules by the emulsion method. A DCM solution of ligand **1** (0.1 mM) and an aqueous solution of $ZnSO_4$ (5.0 mM) were used to synthesize $Zn_2(SO_4)_2(tpy)_2$ CONASH capsules by the liquid–liquid interfacial coordination reaction. The DCM solution and aqueous solution (1:3 v/v) were injected into a test tube and mixed by vigorous shaking at room temperature. The emulsion interface was allowed to stand for 1 h, and the $Zn_2(SO_4)_2(tpy)_2$ CONASH film generated at the interfaces of the emulsion and $Zn_2(SO_4)_2(tpy)_2$ CONASH droplets emerged as light-yellow spheres.

Data availability

The data for the plots in this work and other findings from this study are available from the corresponding author upon reasonable request.

Received: 20 June 2020; Accepted: 13 July 2020
Published online: 14 August 2020

References

1. Han, W., Kawakami, R. K., Gmitra, M. & Fabian, J. Graphene spintronics. *Nat. Nanotechnol.* **9**, 794–807 (2014).
2. Li, L. *et al.* Functionalized graphene for high-performance two-dimensional spintronics devices. *ACS Nano* **5**, 2601–2610 (2011).
3. Eda, G. *et al.* Photoluminescence from chemically exfoliated MoS_2. *Nano Lett.* **11**, 5111–5116 (2011).
4. Mak, K. F. & Shan, J. Photonics and optoelectronics of 2D semiconductor transition metal dichalcogenides. *Nat. Photonics* **10**, 216–226 (2016).
5. Zhang, H. Ultrathin two-dimensional nanomaterials. *ACS Nano* **9**, 9451–9469 (2015).
6. Bauer, T. *et al.* Synthesis of free-standing, monolayered organometallic sheets at the air/water interface. *Angew. Chem. Int. Ed.* **50**, 7879–7884 (2011).
7. Cassabois, G., Valvin, P. & Gil, B. Hexagonal boron nitride is an indirect bandgap semiconductor. *Nat. Photonics* **10**, 262–266 (2016).
8. Burch, K. S., Mandrus, D. & Park, J. G. Magnetism in two-dimensional van der Waals materials. *Nature* **563**, 47–52 (2018).
9. Sakamoto, R. *et al.* Coordination nanosheets (CONASHs): Strategies, structures and functions. *Chem. Commun.* **53**, 5781–5801 (2017).
10. Sakamoto, R. *et al.* The coordination nanosheet (CONASH). *Coord. Chem. Rev.* **320–321**, 118–128 (2016).
11. Kambe, T. *et al.* Redox control and high conductivity of nickel bis(dithiolene) complex π-nanosheet: A potential organic two-dimensional topological insulator. *J. Am. Chem. Soc.* **136**, 14357–14360 (2014).
12. Sun, X. *et al.* Conducting π-conjugated bis(iminothiolato)nickel nanosheet. *Chem. Lett.* **46**, 1072–1075 (2017).
13. Pal, T. *et al.* Interfacial synthesis of electrically conducting palladium bis(dithiolene) complex nanosheet. *ChemPlusChem* **80**, 1255–1258 (2015).
14. Wada, K., Sakaushi, K., Sasaki, S. & Nishihara, H. Multielectron-transfer-based rechargeable energy storage of two-dimensional coordination frameworks with non-innocent ligands. *Angew. Chem. Int. Ed.* **57**, 8886–8890 (2018).
15. Phua, E. J. H. *et al.* Oxidation-promoted interfacial synthesis of redox-active bis(diimino)nickel nanosheet. *Chem. Lett.* **47**, 126–129 (2018).
16. Tsukamoto, T. *et al.* Coordination nanosheets based on terpyridine-zinc(II) complexes: As photoactive host materials. *J. Am. Chem. Soc.* **139**, 5359–5366 (2017).
17. Sakamoto, R. *et al.* Photofunctionality in porphyrin-hybridized bis(dipyrrinato)zinc(II) complex micro- and nanosheets. *Angew. Chem. Int. Ed.* **56**, 3526–3530 (2017).
18. Sun, X. *et al.* Bis(aminothiolato)nickel nanosheet as a redox switch for conductivity and an electrocatalyst for the hydrogen evolution reaction. *Chem. Sci.* **8**, 8078–8085 (2017).
19. Zhou, D. *et al.* SiO_2 hollow nanosphere-based composite solid electrolyte for lithium metal batteries to suppress lithium dendrite growth and enhance cycle life. *Adv. Energy Mater.* **6**, 1502214 (2016).
20. Jeong, G. Y. *et al.* Bioactive MIL-88A framework hollow spheres via interfacial reaction in-droplet microfluidics for enzyme and nanoparticle encapsulation. *Chem. Mater.* **27**, 7903–7909 (2015).
21. Guan, C. *et al.* Hollow Co_3O_4 nanosphere embedded in carbon arrays for stable and flexible solid-state zinc-air batteries. *Adv. Mater.* **29**, 1704117 (2017).
22. Xia, X. H., Tu, J. P., Wang, X. L., Gu, C. D. & Zhao, X. B. Mesoporous Co_3O_4 monolayer hollow-sphere array as electrochemical pseudocapacitor material. *Chem. Commun.* **47**, 5786–5788 (2011).
23. Furukawa, S., Reboul, J., Diring, S., Sumida, K. & Kitagawa, S. Structuring of metal-organic frameworks at the mesoscopic/macroscopic scale. *Chem. Soc. Rev.* **43**, 5700–5734 (2014).
24. Liang, Z. *et al.* A protein@metal–organic framework nanocomposite for pH-triggered anticancer drug delivery. *Dalton Trans.* **47**, 10223–10228 (2018).
25. Xu, Z. *et al.* Encapsulation of hydrophobic guests within metal–organic framework capsules for regulating host–guest interaction. *Chem. Mater.* **32**, 3553–3560 (2020).
26. Kandambeth, S. *et al.* Self-templated chemically stable hollow spherical covalent organic framework. *Nat. Commun.* **6**, 6786 (2015).
27. Lu, Z. *et al.* A hollow microshuttle-shaped capsule covalent organic framework for protein adsorption. *J. Mater. Chem. B* **7**, 1469–1474 (2019).
28. Guo, J. *et al.* Engineering multifunctional capsules through the assembly of metal-phenolic networks. *Angew. Chem. Int. Ed.* **53**, 5546–5551 (2014).
29. Ameloot, R. *et al.* Interfacial synthesis of hollow metal-organic framework capsules demonstrating selective permeability. *Nat. Chem.* **3**, 382–387 (2011).
30. Wu, S., Xin, Z., Zhao, S. & Sun, S. High-throughput droplet microfluidic synthesis of hierarchical metal-organic framework nanosheet microcapsules. *Nano Res.* **12**, 2736–2742 (2019).
31. Wang, B. *et al.* Macroporous materials: Microfluidic fabrication, functionalization and applications. *Chem. Soc. Rev.* **46**, 855–914 (2017).
32. Mondal, S., Yoshida, T. & Higuchi, M. Electrochromic devices using Fe(II)-based metallo-supramolecular polymer: Introduction of ionic liquid as electrolyte to enhance the thermal stability. *J. Soc. Inf. Disp.* **27**, 661–666 (2019).
33. Takada, K. *et al.* Electrochromic bis(terpyridine)metal complex nanosheets. *J. Am. Chem. Soc.* **137**, 4681–4689 (2015).
34. Maeda, H., Sakamoto, R. & Nishihara, H. Interfacial synthesis of electrofunctional coordination nanowires and nanosheets of bis(terpyridine) complexes. *Coord. Chem. Rev.* **346**, 139–149 (2017).
35. Jiang, T. *et al.* Dimethoxy triarylamine-derived terpyridine-zinc complex: A fluorescence light-up sensor for citrate detection based on aggregation-induced emission. *J. Mater. Chem. C* **4**, 10040–10046 (2016).
36. Bode, G., Lade, M. & Schomäcker, R. The kinetics of an interfacial reaction in microemulsions with excess phases. *Chem. Eng. Technol.* **23**, 405–409 (2000).

37. Piradashvili, K., Alexandrino, E. M., Wurm, F. R. & Landfester, K. Reactions and polymerizations at the liquid-liquid interface. *Chem. Rev.* **116**, 2141–2169 (2016).
38. Soma, J. & Papadopoulos, K. D. Ostwald ripening in sodium dodecyl sulfate-stabilized decane-in-water emulsions. *J. Colloid Interface Sci.* **181**, 225–231 (1996).
39. Lin, Y., Ng, K. M., Chan, C. M., Sun, G. & Wu, J. High-impact polystyrene/halloysite nanocomposites prepared by emulsion polymerization using sodium dodecyl sulfate as surfactant. *J. Colloid Interface Sci.* **358**, 423–429 (2011).
40. Liu, J. *et al.* Highly water-dispersible biocompatible magnetite particles with low cytotoxicity stabilized by citrate groups. *Angew. Chem. Int. Ed.* **48**, 5875–5879 (2009).
41. Christopher, G. F. & Anna, S. L. Microfluidic methods for generating continuous droplet streams. *J. Phys. D. Appl. Phys.* **40**, 437–446 (2017).
42. Garstecki, P., Fuerstman, M. J., Stone, H. A. & Whitesides, G. M. Formation of droplets and bubbles in a microfluidic T-junction—Scaling and mechanism of break-up. *Lab Chip* **6**, 437–446 (2006).
43. Cavazzini, M. *et al.* Synthesis, characterization, absorption spectra, and luminescence properties of multinuclear species made of Ru(II) and Ir(III) chromophores. *Inorg. Chem.* **48**, 8578–8592 (2009).

Acknowledgements

This work was financially supported by JST-CREST JPMJCR15F2, and JSPS KAKENHI Grant Number 19H05460 for H.N, and the China Scholarship Council (No. 201706795025) for M.L.

Author contributions

H.N. conceived the research. R.A., M.L. and R.T. designed the experiments and prepared the samples. R.A and M.L. performed the measurements of $Fe(tpy)_2$ CONASH capsules and $Zn_2(SO_4)_2(tpy)_2$ CONASH capsules, respectively. H.M. contributed to the electrochemical measurements. All authors discussed the results. R.A. wrote the paper with input from all authors. H.M., M.L., R.T. and H.N. revised the manuscript.

Competing interests

The authors declare no competing interests.

Additional information

Supplementary information is available for this paper at https://doi.org/10.1038/s41598-020-70715-6.

Correspondence and requests for materials should be addressed to H.N.

Reprints and permissions information is available at www.nature.com/reprints.

Publisher's note Springer Nature remains neutral with regard to jurisdictional claims in published maps and institutional affiliations.